CENTRAL RESEARCH LIBRARY
DOCUMENT COLLECTION

OAK RIDGE NATIONAL LABORATORY
operated by
UNION CARBIDE CORPORATION
NUCLEAR DIVISION
for the
U.S. ATOMIC ENERGY COMMISSION

ORNL-TM-3514

MARTIN MARIETTA ENERGY SYSTEMS LIBRARIES
3 4456 0251274 2

cy .45

DATE - October 5, 1971

Neutron Physics Division

EXPERIMENTAL INVESTIGATION OF NEUTRON STREAMING THROUGH THE GRID-PLATE SHIELD OF THE FAST FLUX TEST FACILITY

Written by:

C. E. Clifford
F. R. Mynatt
P. N. Stevens*

Work done by:

R. M. Freestone, Jr.
M. L. Gritzner
K. M. Henry
L. B. Holland
J. L. Hull
J. Lewin
J. J. Manning
J. N. Money
F. J. Muckenthaler
F. R. Mynatt

Abstract

An experiment was performed at the Tower Shielding Facility (TSF) to determine the effect of neutron streaming in sodium coolant holes on the peak neutron fluence transmitted through a prototype of the FTR grid-plate shield. Three grid-plate shield configurations, supplied by WADCO Corporation, a subsidiary of Westinghouse Electric Corporation, were used in the experiment, each having different hole configurations. A flux increase of about 10% was measured for straight-through holes and a 3% increase was measured for holes having a single offset. Standard deviations of measurements obtained were approximately 2%.

*Present address: Oregon State University, Radiation Center, Corvallis, Oregon 97331

OAK RIDGE NATIONAL LABORATORY
CENTRAL RESEARCH LIBRARY
DOCUMENT COLLECTION
LIBRARY LOAN COPY
DO NOT TRANSFER TO ANOTHER PERSON
If you wish someone else to see this document, send in name with document and the library will arrange a loan.
UCN-7969
(3 3-67)

This report was prepared as an account of work sponsored by the United States Government. Neither the United States nor the United States Atomic Energy Commission, nor any of their employees, nor any of their contractors, subcontractors, or their employees, makes any warranty, express or implied, or assumes any legal liability or responsibility for the accuracy, completeness or usefulness of any information, apparatus, product or process disclosed, or represents that its use would not infringe privately owned rights.

TABLE OF CONTENTS

		Page
LIST OF FIGURES		v
LIST OF TABLES		vii
I.	INTRODUCTION	1
II.	EXPERIMENTAL CONFIGURATION	2
III.	INSTRUMENTATION	17
IV.	RESULTS	18
	MODIFIED SPECTRUM	18
	GRID-PLATE SHIELD INSERTS	24
	UNCOUPLED REACTOR-SPECTRUM-MODIFIER ARRANGEMENT	34
V.	SUMMARY	36

MARTIN MARIETTA ENERGY SYSTEMS LIBRARIES

3 4456 0251274 2

LIST OF FIGURES

Page

Fig. 1. Experimental Configuration No. 1 For Spectral Modifier Neutron Transmission Measurement 3

Fig. 2. Modified Spectral Modifier Configuration No. 1 for the NE-213 Measurements 4

Fig. 3. Stainless-Steel Filler Plates for Grid-Plate Shield Mockup Showing Configuration of Coolant Holes 5

Fig. 4. Array of Filler Plates for Grid-Plate Shield Mockup . 6

Fig. 5. Coolant Hole Configuration for Grid-Plate Shield for Insert No. 1. 7

Fig. 6. Coolant Hole Configuration for Grid-Plate Shield For Insert No. 2 (contains Y-shaped slots). 8

Fig. 7. Coolant Hole Configuration For Grid-Plate Shield For Insert No. 3. 9

Fig. 8. Stainless-Steel and Aluminum Collar Shield Which Contained Grid-Plate Shield Inserts 10

Fig. 9. Top View of Collar Shield Showing Mid-Plane Offset. . 11

Fig. 10. Configuration No. 2, Spectral Modifier and Grid-Plate Shield Mockup Arrangement 13

Fig. 11. Lucite Detector Collimator Having the "O" Hole Configuration 14

Fig. 12. Lucite Detector Collimator Having the "Y" Hole Configuration 15

Fig. 13. Configuration No. 3, Spectral Modifier and Grid-Plate Shield Arrangement With the Reactor Decoupled 16

I. INTRODUCTION

A lower axial shield is required to reduce the neutron fluence incident on the FTR core support grid plate to insure that a reasonable (10 years) lifetime is obtained. The purpose of this series of experiments performed at the Tower Shielding Facility (TSF) was to determine the relative importance of neutron streaming through holes penetrating a prototype of the grid-plate shield. These holes must be provided to allow passage of the sodium coolant from the lower plenum up through the fuel elements. The grid-plate shield is fabricated in the lower end of each fuel assembly and consists of stainless-steel blocks ∿ 1-in. thick which are perforated by six holes approximately 0.5 in. in diameter. This arrangement was chosen in order to allow flexibility in the orificing of the individual fuel elements. Pressure-drops through the grid-plate shield can be readily varied, depending on the degree of alignment of the holes throughout the 22-in.-thick grid-plate shield region. Three grid-plate shield samples were provided by WADCO for this experiment and had various degrees of alignment between the holes. These samples were placed in a spectrum which was adjusted to simulate as closely as possible the spectrum incident on the FTR grid-plate shield as predicted by calculations with the two-dimensional discrete ordinates code DOT. Measurements of the total neutron flux were taken just below the grid-plate shield in order to determine the degree of neutron streaming associated with the various configurations of holes. These measurements were taken both with and without a collimator for the neutron detector. The collimator holes matched those in the shield and attenuated the streaming effects. Measurements were repeated at least three times for each configuration measured in an attempt to insure an

accuracy of 5% or less in the experimental measurements. This accuracy was required to insure that a streaming factor as small as 1.35 could readily be detected.

II. EXPERIMENTAL CONFIGURATION

The source of neutrons for these experiments was the TSF-SNAP reactor[1-3] which was placed above a laminated slab designed to modify the shape of the leakage spectrum of the SNAP reactor to that of the spectrum incident on the FTR grid-plate shield. The spectrum modifier consisted of a 10-in.-thick stainless-steel layer followed by a 1-in.-thick polyethylene slab and a 1/4-in.-thick boral sheet. The reactor and spectrum modifier are shown in Fig. 1, as well as the position of the Bonner ball detectors. Count rates were obtained for nine different Bonner balls in the location shown. Since each of these detectors has a different energy-dependent response function, a calculation which correctly predicts the counting rates of all nine detectors can be assumed to be reasonably accurate. In addition to the Bonner ball detectors, neutron spectra were also measured with the Benjamin spectrometer which covered the energy range from 0.05 to 1.5 MeV. The spherical hydrogen-filled proportional counter, which is the detector for the Benjamin-type spectrometer, is considerably less sensitive than the Bonner balls and was therefore located at a position closely adjacent to the lower surface of the spectrum modifier. In order to reduce the gamma-ray intensity for NE-213 spectrometer measurements, a zirconium gamma-ray shield was added to the configuration, as shown in Fig. 2.

The configuration of grid-plate shield mockups is shown in Figs. 3-9. Figure 3 shows a top view of the hole arrangement of the individual plates in the mockup. Also shown are the Y-shaped slots which represent the

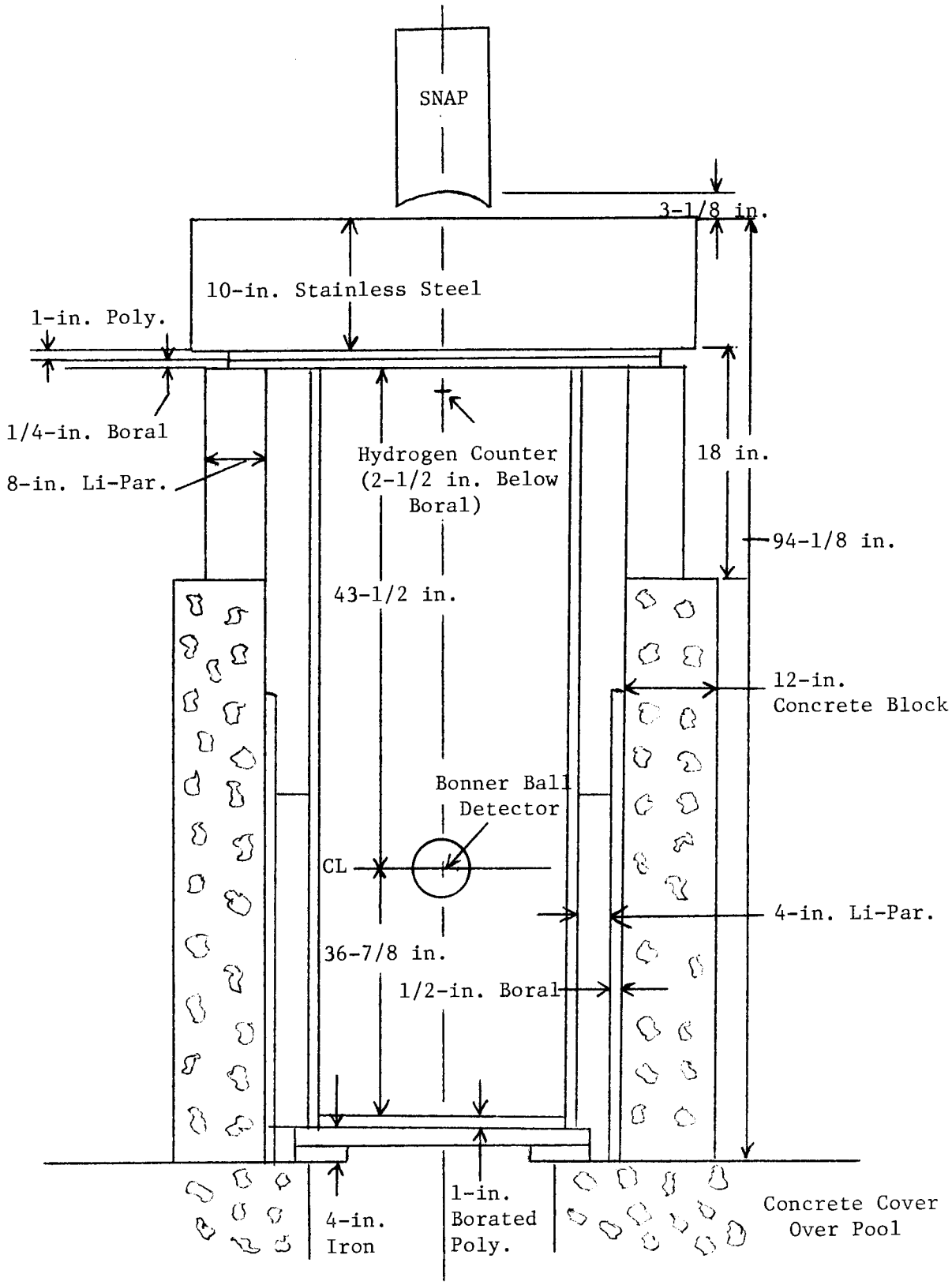

Fig. 1. Experimental Configuration No. 1 For Spectral Modifier Neutron Transmission Measurement.

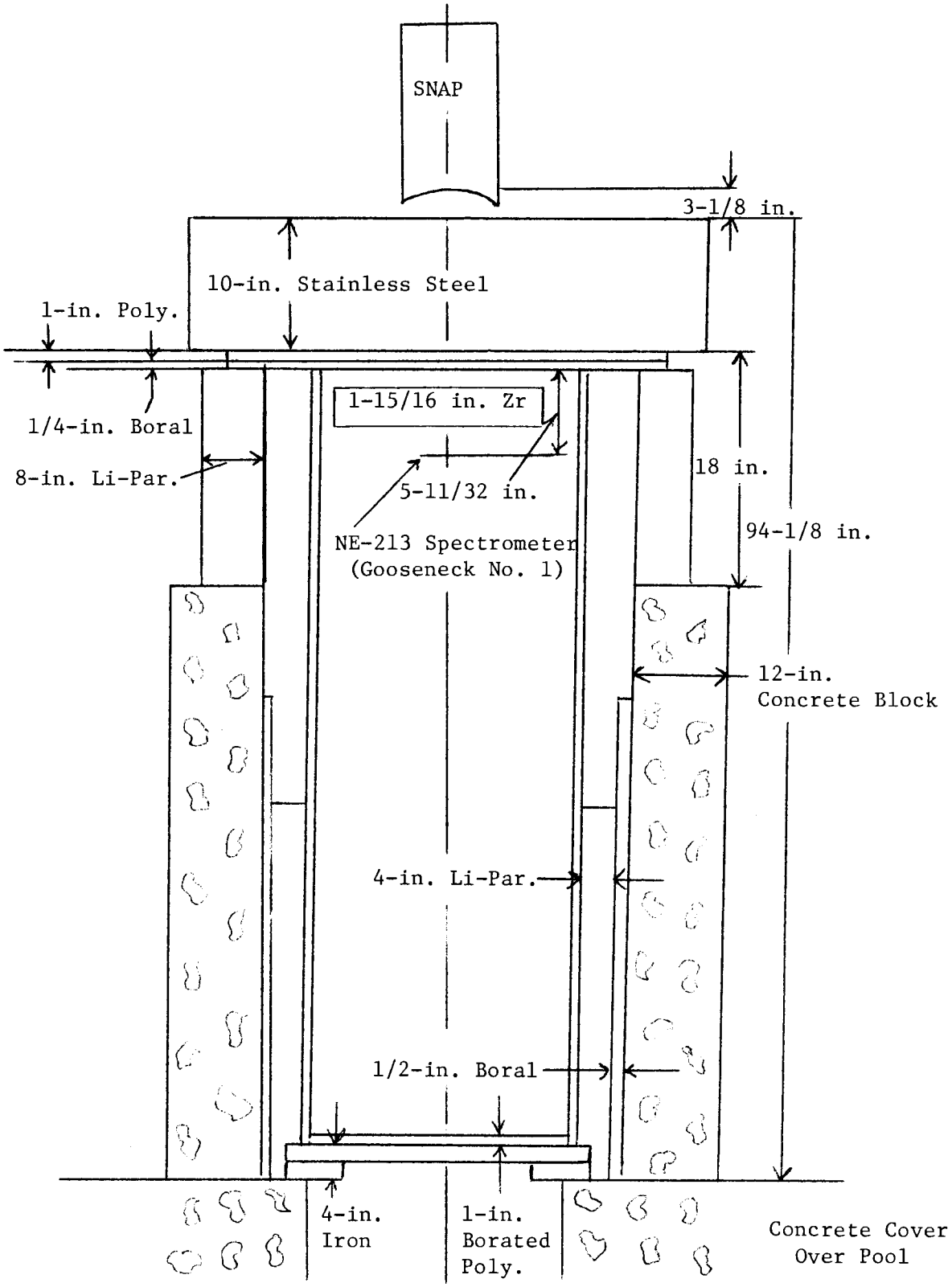

Fig. 2. Modified Spectral Modifier Configuration No. 1 for the NE-213 Measurements.

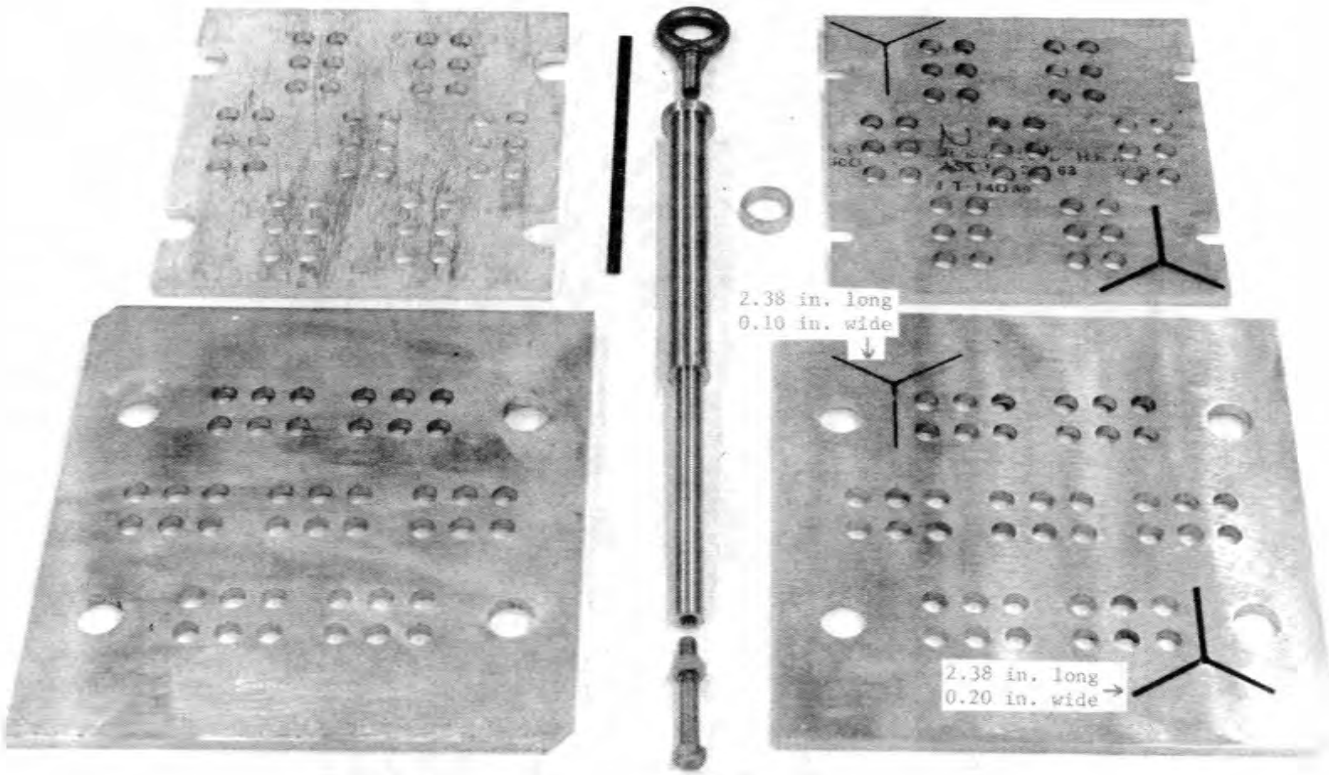

Fig. 3. Stainless-Steel Filler Plates for Grid-Plate Shield Mockup Showing Configuration of Coolant Holes.

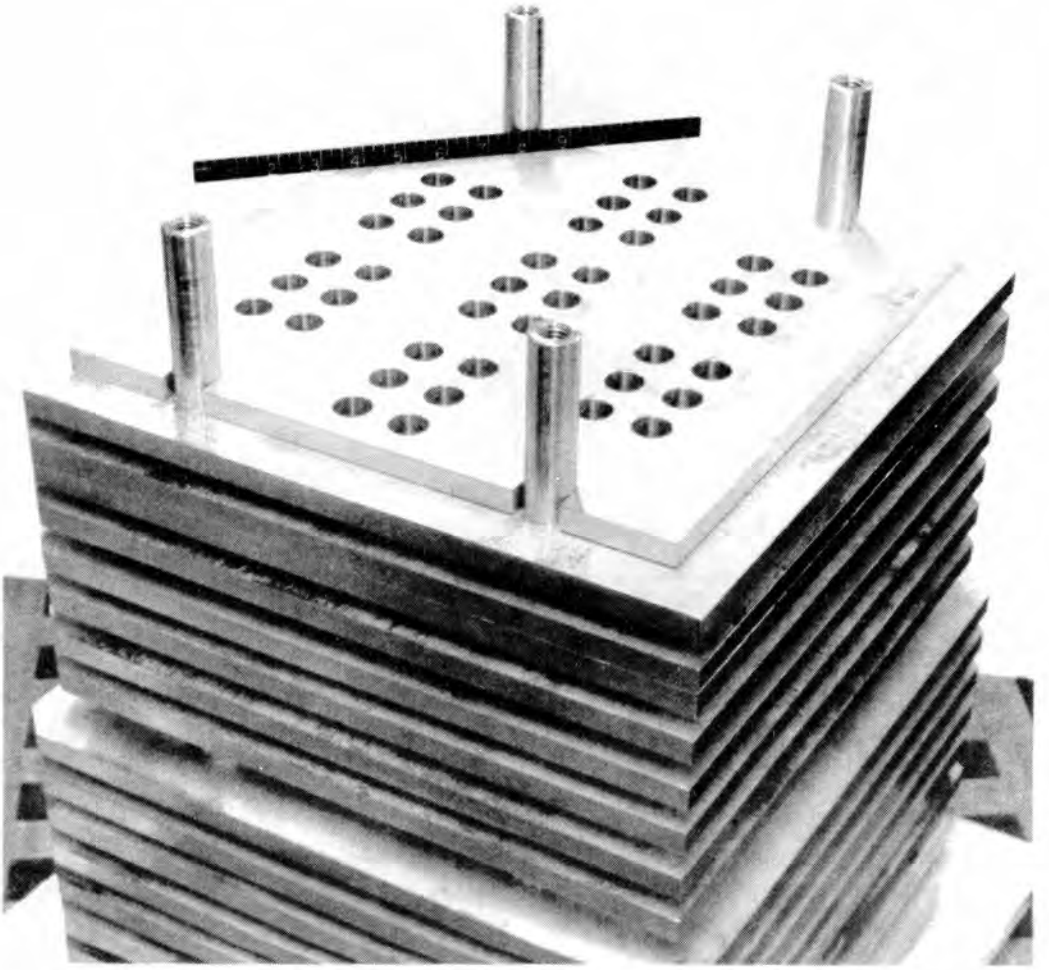

Fig. 4. Array of Filler Plates for Grid-Plate Shield Mockup.

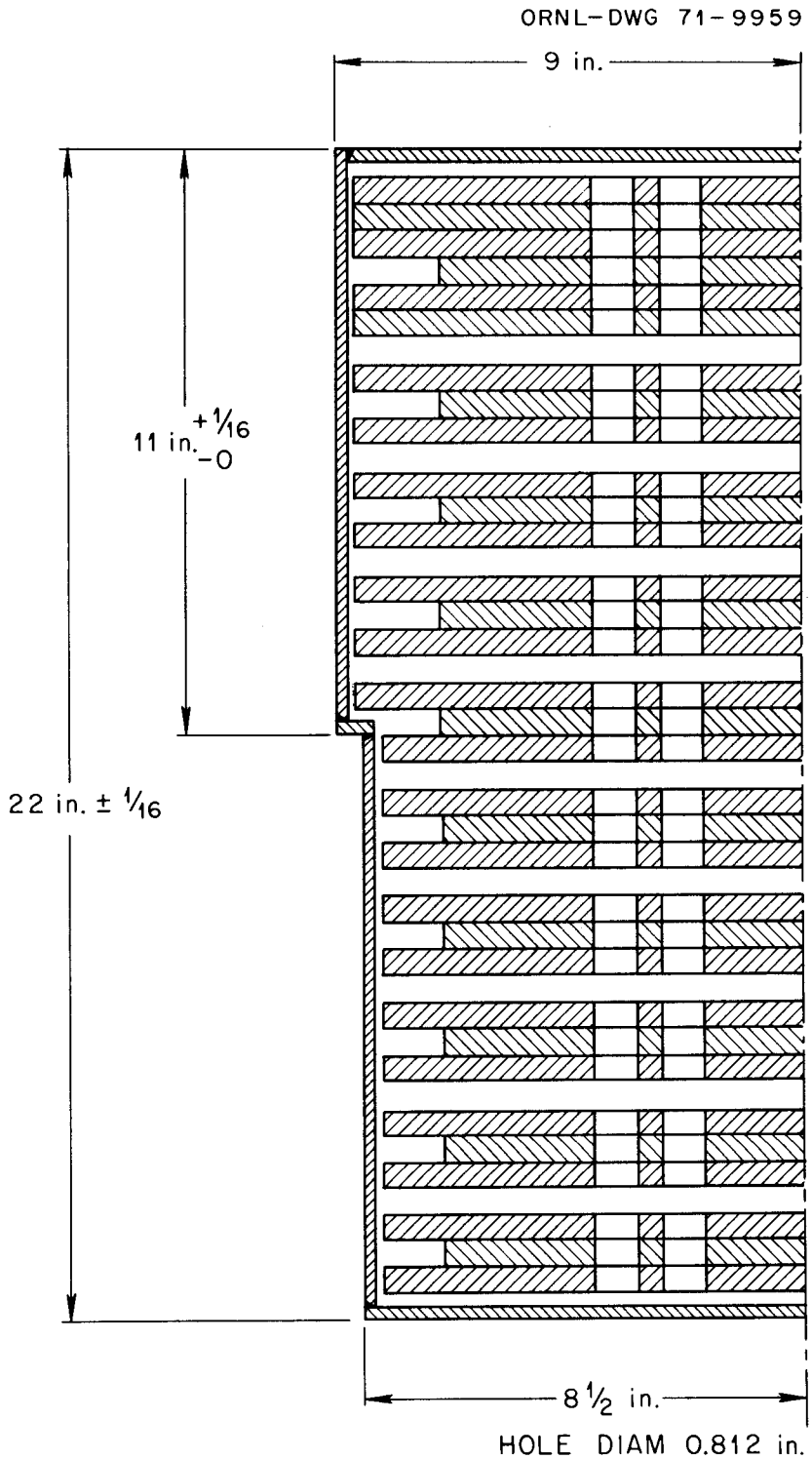

Fig. 5. Coolant Hole Configuration for Grid-Plate Shield for Insert No. 1

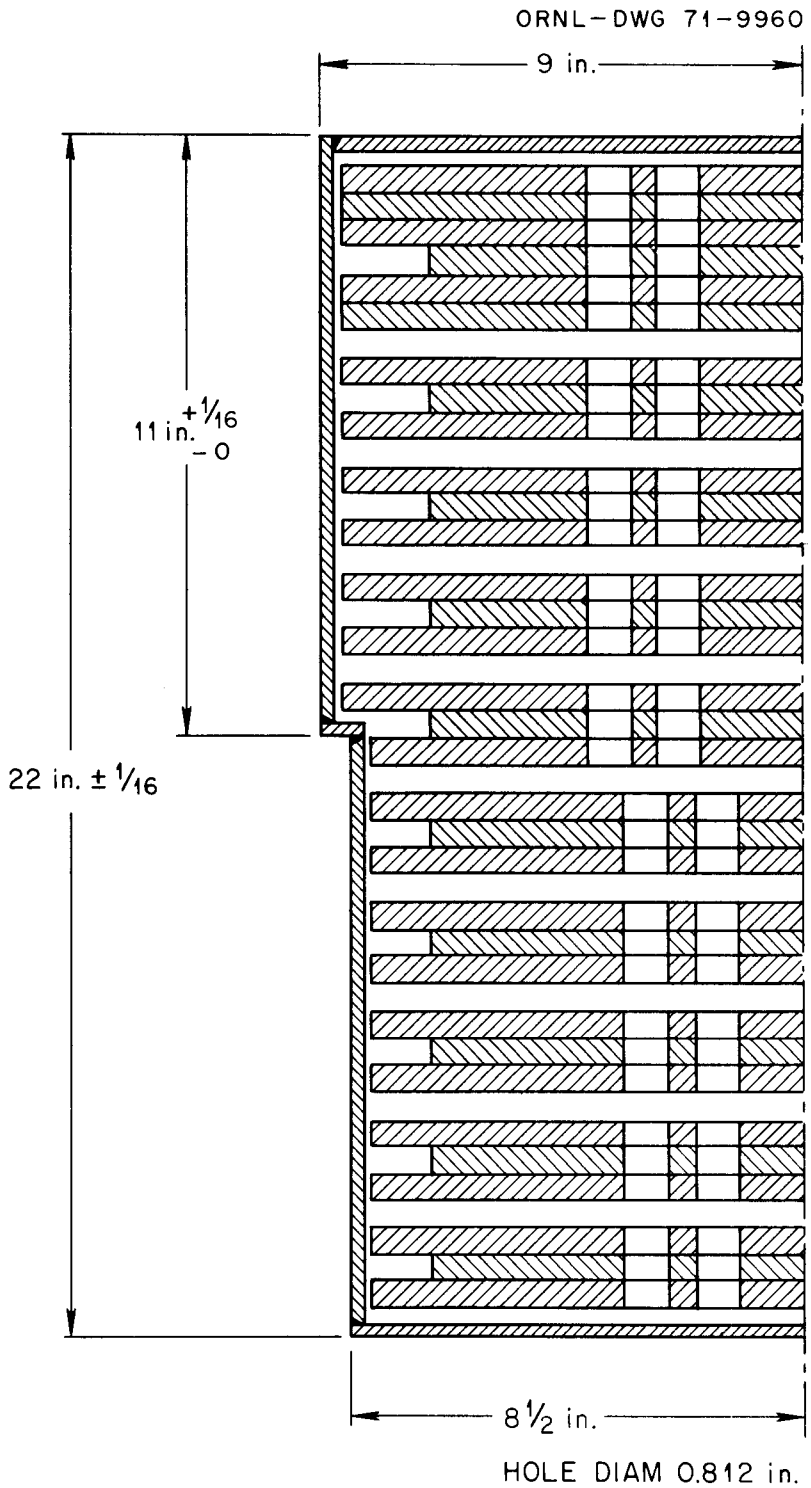

Fig. 6. Coolant Hole Configuration for Grid-Plate Shield for Insert No. 2 (contains Y-shaped slots).

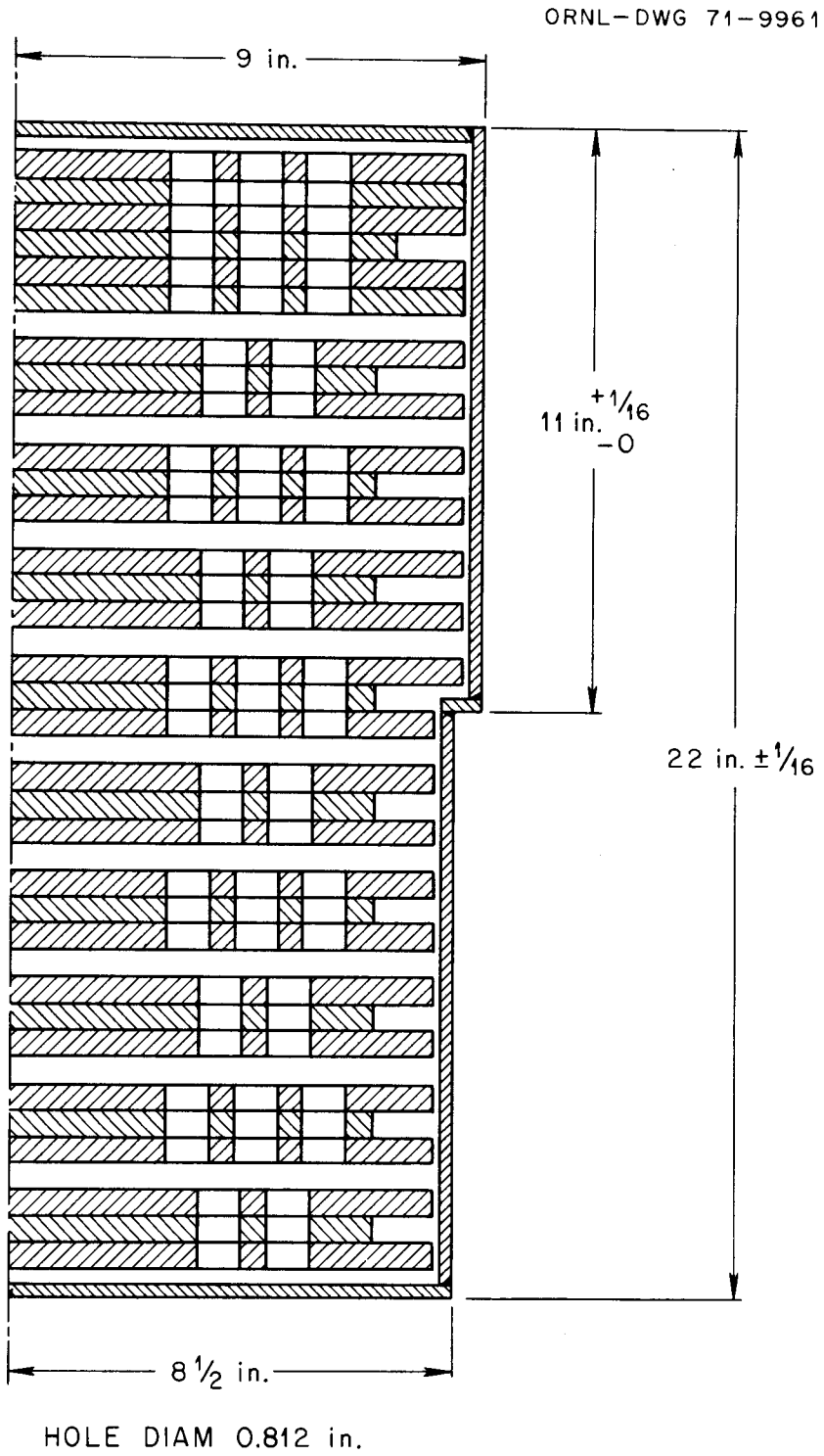

Fig. 7. Coolant Hole Configuration for Grid-Plate Shield for Insert No. 3.

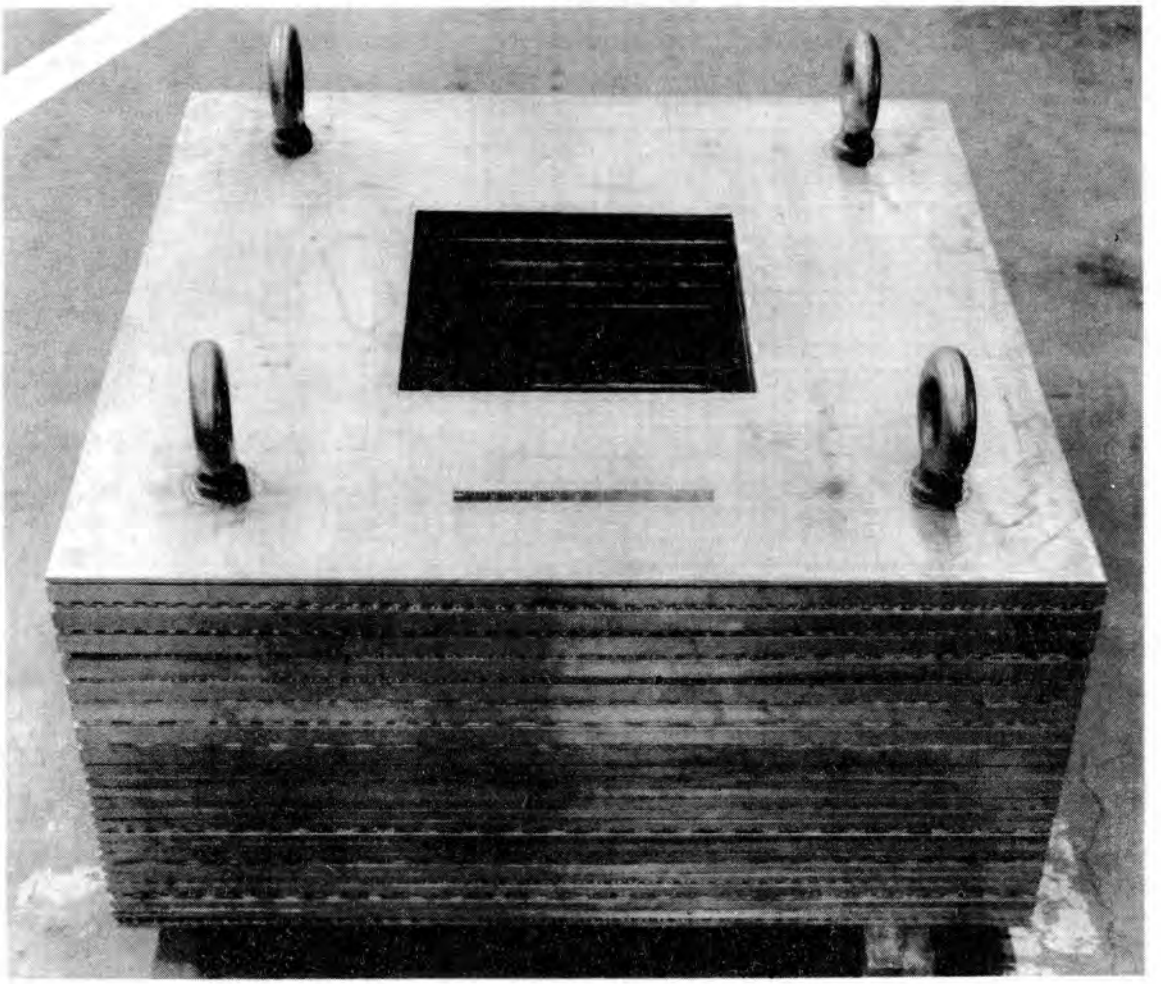

Fig. 8. Stainless-Steel and Aluminum Collar Shield Which Contained Grid-Plate Shield Inserts.

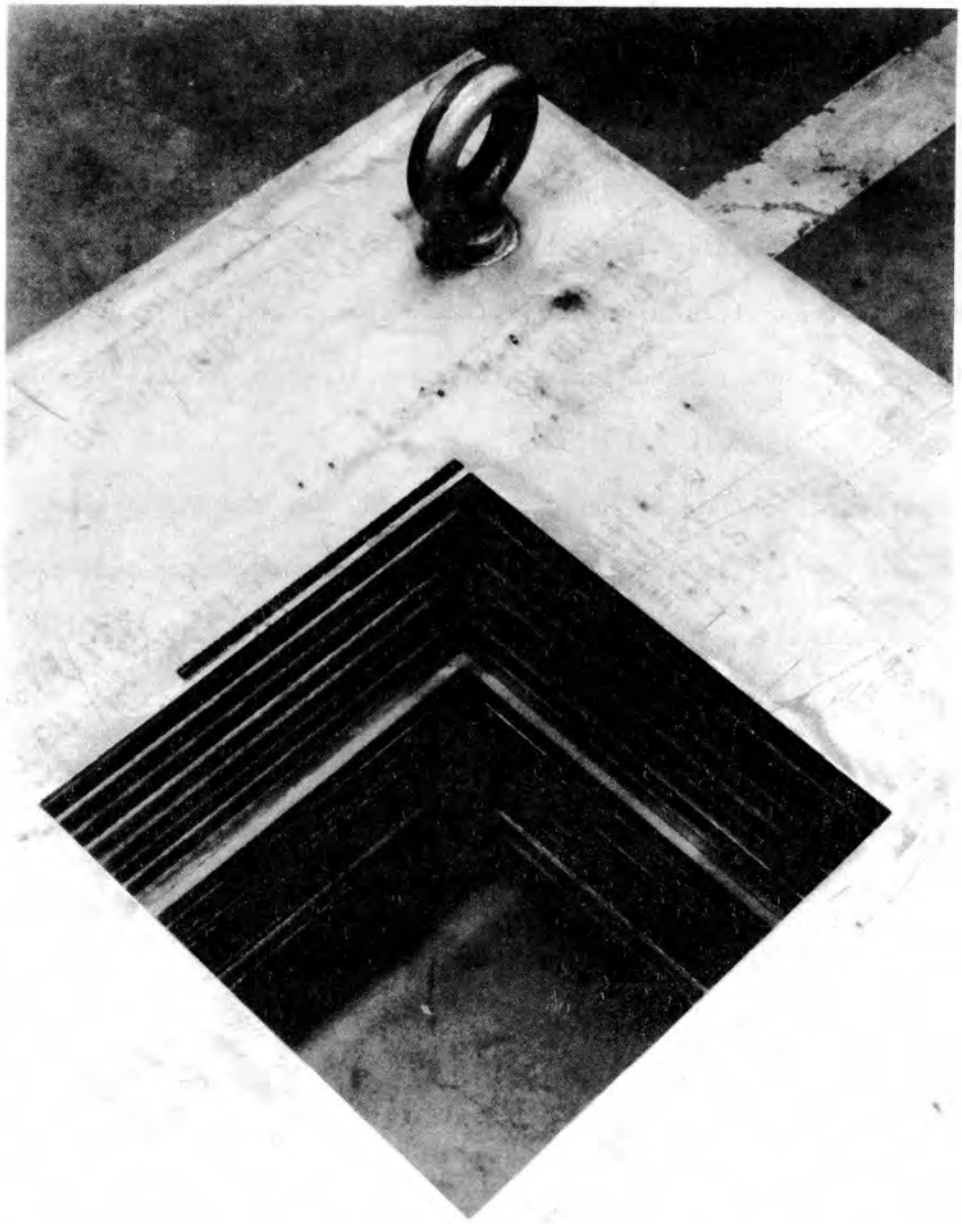

Fig. 9. Top View of Collar Shield Showing Mid-Plane Offset.

clearance gap between the hexagonal fuel element assemblies. The smaller plates shown are in the lower section of the grid-plate shield insert which is stepped in order to avoid neutron streaming along the sides of the insert. Figure 4 is a photograph of the assembly of plates.

Figures 5-7 show elevations of the three assemblies and indicate the degree of hole alignment in each. Figures 8 and 9 are photographs of the stainless-steel-aluminum collar which surrounded the grid-plate shield assemblies. Each aluminum plate was perforated to reduce its dens density to $\sim$ 1.6 gm/cc.

Configuration no. 2, shown in Fig. 10, was the basic experimental setup used for all the grid-plate shield transmission measurements. Figure 10 shows a 4-in.-thick lucite collimator placed beneath the shield insert and collar which contains 0.812-in.-diam. holes and Y-shaped slots which match those in the grid-plate shield mockup. Figures 11 and 12 are photographs of the O and Y collimators, respectively. The only significant difference between configurations 1 and 2 is the inclusion of the prototype shield (collar-insert arrangement).

Configuration no. 3, shown in Fig. 13, provided a reactor-spectrum-modifier arrangement more amenable to analysis. The reactivity coupling between the SNAP reactor system and the spectrum modifier (reflector), which exists in configurations 1 and 2, would significantly complicate the corresponding analysis.

The various grid-plate shield geometric arrangements were realized by a collar-insert arrangement, as shown in Figs. 10 and 13. The three grid-plate shield configurations tested will be referred to as inserts 1, 2, and 3, and will consist of material (stainless steel and sodium)

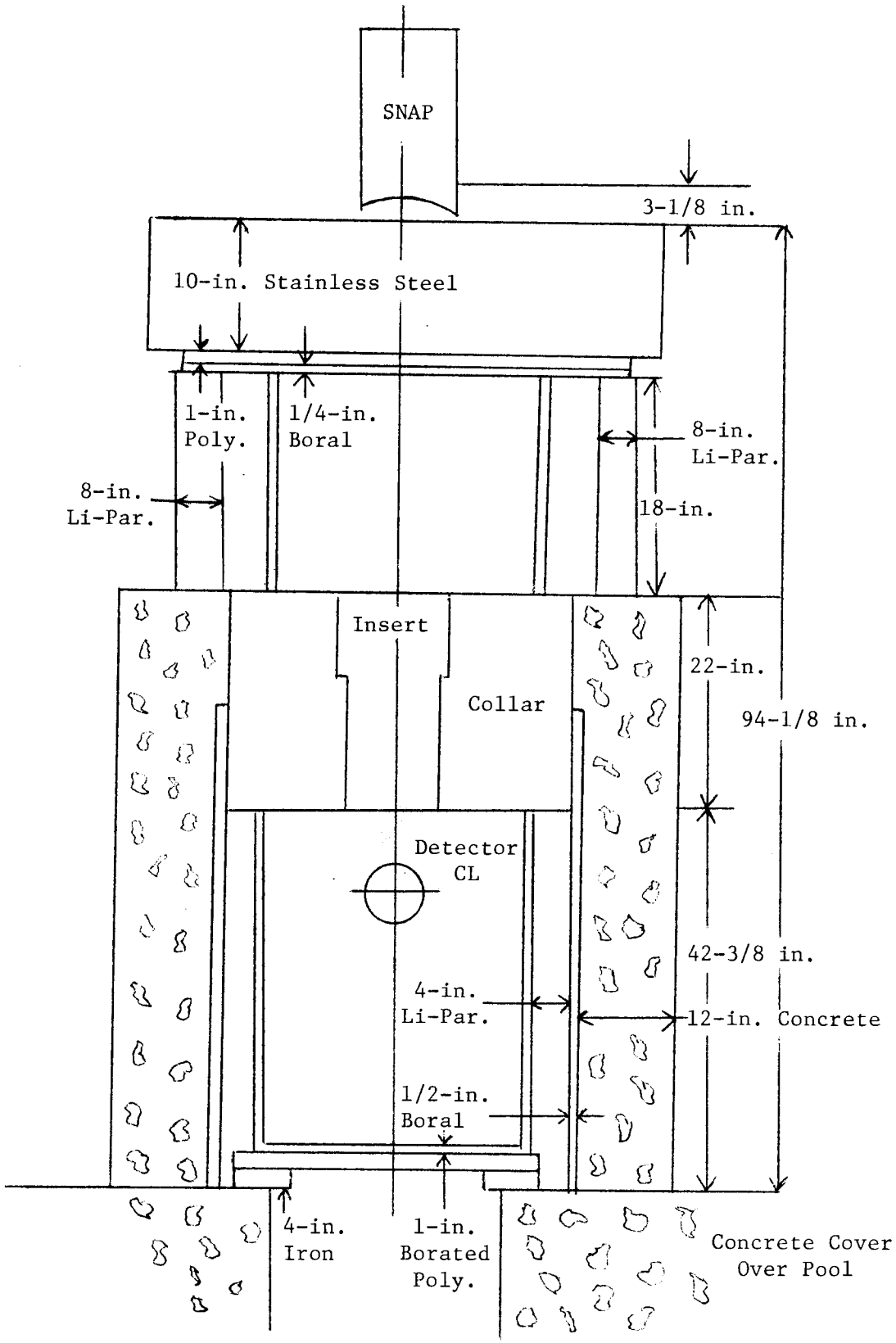

Fig. 10. Configuration No. 2, Spectral Modifier and Grid-Plate Shield Mockup Arrangement.

PHOTO 1759-71

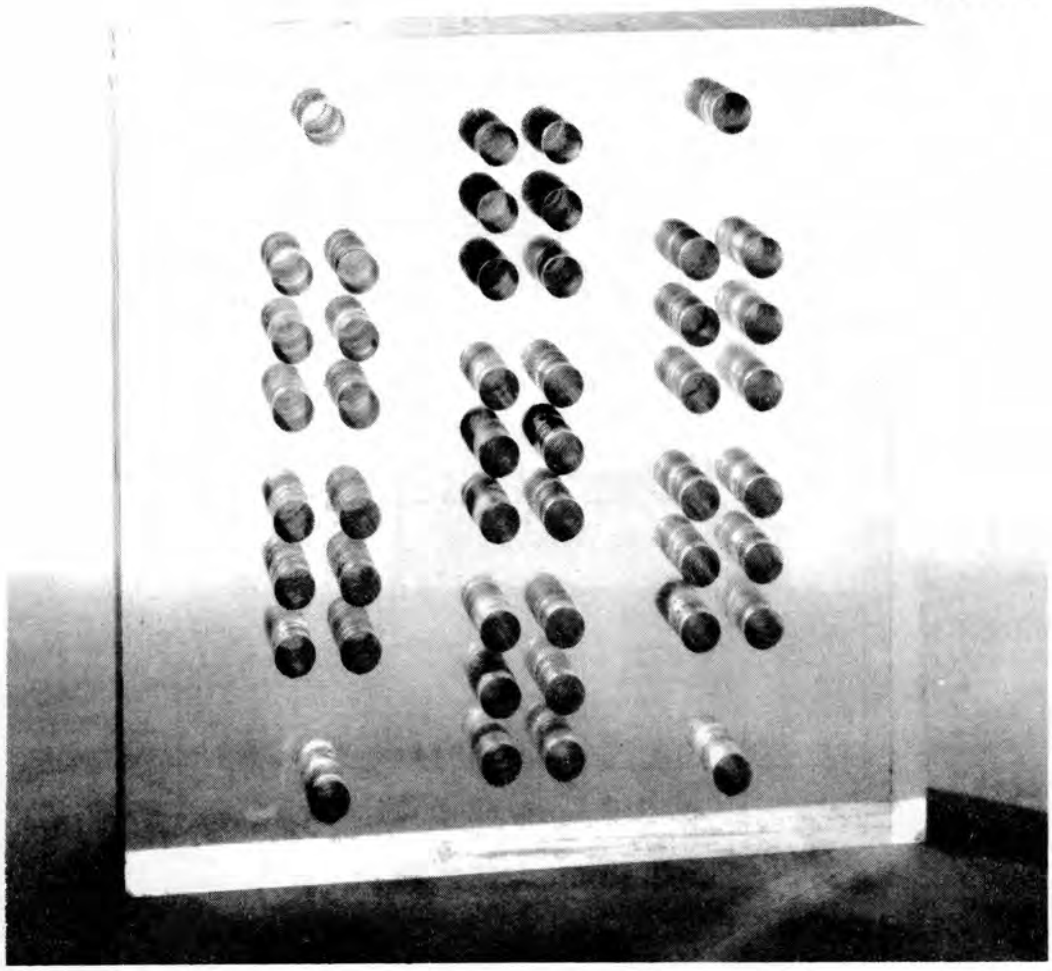

Fig. 11. Lucite Detector Collimator Having the "O" Hole Configuration.

PHOTO 1758-71

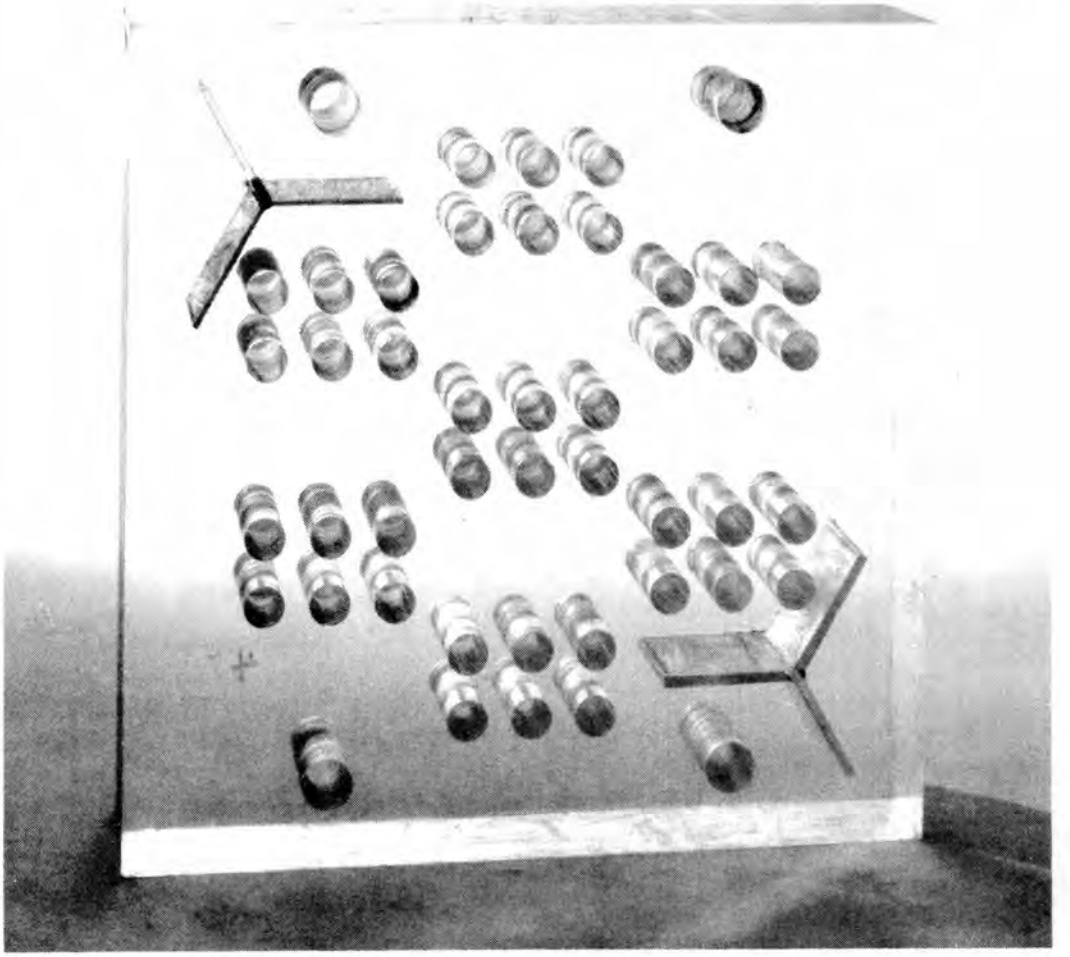

Fig. 12. Lucite Detector Collimator Having the "Y" Hole Configuration.

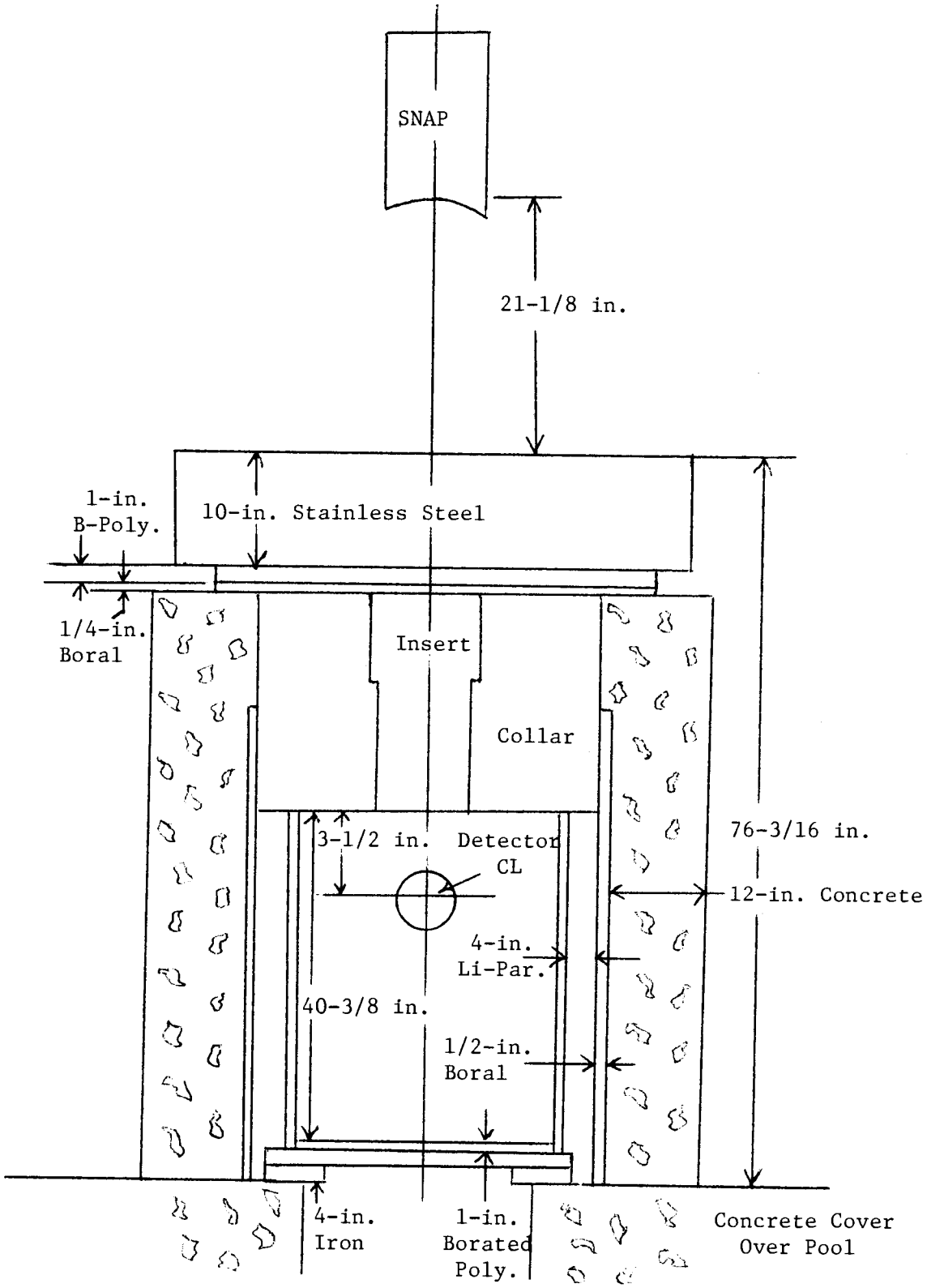

Fig. 13. Configuration No. 3, Spectral Modifier and Grid-Plate Shield Arrangement With the Reactor Decoupled.

arrangements that correspond to straight-through coolant passages (insert no. 1), coolant passages with a single offset (insert no. 2), and an essentially homogeneous arrangement of materials (insert no. 3) obtained using the maximum number of possible offsets. Insert no. 2 also contains two straight-through Y slots, which represent two different sizes for the gaps between the shield subassemblies.

Transmission measurements were performed with and without a lucite detector collimator placed on the emergent face of the grid-plate shield. The Y collimator matches the exit hole pattern in shield inserts 2 and 3 and the 0 collimator matches the exit hole pattern in shield insert 1. These collimators were used to emphasize the effects of the holes and Y slots so as to measure the maximum streaming effects.

III. INSTRUMENTATION

Most of the measurements utilized the 5-in.-diam. Bonner ball counter. The Bonner ball counter consists of a BF_3 thermal-neutron counter surrounded by polyethylene spheres of various sizes. The sensitivity ("counting efficiency" as a function of neutron energy) is significantly different for each of the polyethylene spheres and provides the basis for using the Bonner ball counter as a very crude spectrometer.[4] The present ORNL version of the Bonner ball counter includes the following configurations: bare and cadmium-covered detectors and 3-, 4-, 5-, 6-, 8-, 10-, and 12-in.-diam. polyethylene spheres.

An individual measurement (a certain count rate for a given polyethylene sphere) can be regarded as a property of the radiation field. For example, the response of a 10-in. sphere has been considered proportional to the fast-neutron dose, and here, in this program, the 5-in. Bonner ball

configuration was used as a total-fluence detector. This follows since the 5-in. sphere has a relatively flat response function, as shown in Fig. 14.

Two additional spectral measurements were taken of the radiation emergent from the spectrum modifier - configuration no. 1. These measurements involved the modified Benjamin spectrometer[5] (70 keV to 1.2 MeV) and the NE-213 spectrometer[6] (0.8 MeV to 12.2 MeV). The Benjamin spectrometer uses three spherical recoil-proton proportional counters, and the NE-213 spectrometer uses an organic recoil-proton scintillator coupled with a photomultiplier tube.

IV. RESULTS

The various experimental setups (combinations of configuration, insert, and collimator) are presented in Table 1. Where repeat measurements were taken, a fractional standard deviation associated with the average was calculated. Since enough counts were taken for all runs (greater than 30,000 counts), counting statistics were negligible, and the fractional standard deviation, as reported here,is characteristic of the reproducibility of the experimental setup.

Modified Spectrum - The emergent radiation from the SNAP reactor was modified to provide the desired source spectrum. Run no. 1 is a measurement of the spectrum and total flux incident on the test shield specimen. Results are presented in Table 2 as (cpm/W) for the complete set of Bonner ball configurations. Additional spectral measurements were taken with the hydrogen counter and the NE-213 spectrometer, run nos. 8 and 9. The unfolded hydrogen counter spectrum and NE-213 spectrum are plotted in Figs. 15 and 16, respectively. Also shown on these plots are

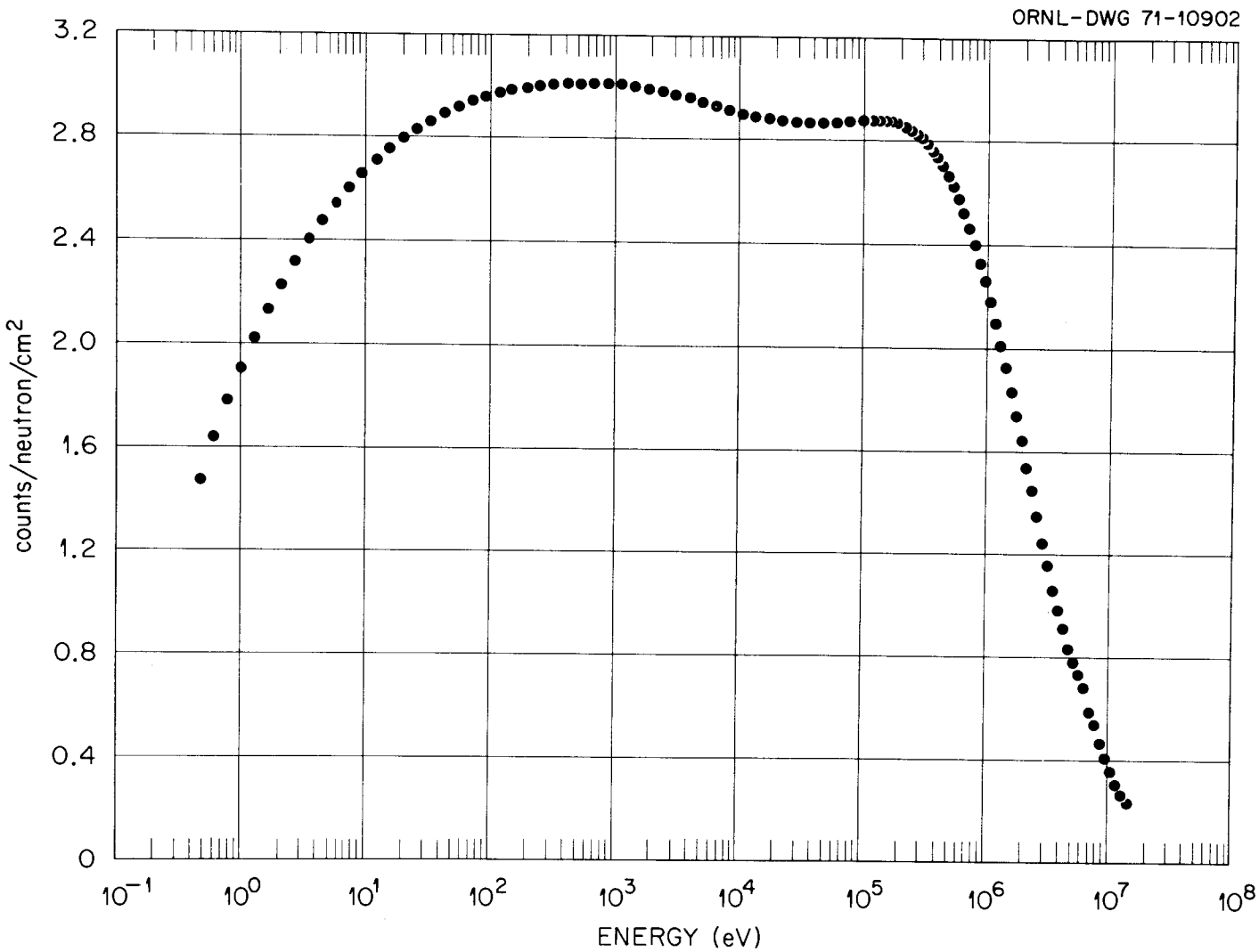

Fig. 14. Bonner Sphere Response For an Isotropic Incident Flux.

Table 1. Experimental Setups

Run	Configuration No.	Insert No.	Collimator	Measurements Taken	Table No.
1	1	None	None	Spectrum and total fluence on centerline	2
2	2	1	O, O(H_2O), Y, None	Total fluence on centerline	3
3	2	2	O, Y, None	Total fluence on centerline and on corners	4
4	2	3	O, Y, Y(H_2O), None	Total fluence on centerline and on corners	5
5	2	3	Y, Y(H_2O)	5-in. Bonner ball traverse	6
6	2	3	None	5-in. Bonner ball traverse	7
7	3	3	None	Total fluence on centerline	8
8	1	None	None	Hydrogen counter spectral measurement	
9	1 (modified)	None	None	NE-213 spectral measurements	

Table 2. Bonner Ball Spectral Measurements on Centerline 43-1/2 in. Below Bottom of SNAP Spectrum Modifier[a] for Configuration #1 With No Insert or Collar, Run #1

Detector[b]	Foreground	Background[c]	Background[d]
	(counts/minute/watt)		
Bare ball	343195	-	33883
Cd-covered	47608	-	637
Cd-covered	45997	-	-
3-in. ball	773560	-	6345
3-in. ball	755493	-	-
4-in. ball	1846450	-	-
5-in. ball	2259897	334020	13862
5-in. ball	2242436	-	-
6-in. ball	2144601	-	-
8-in. ball	1404846	168506	7487
8-in. ball	1394554	-	-
10-in. ball	703467	-	-
12-in. ball	315454	-	-

[a]Same separation used during measurements with inserts and no collimator; i.e., 3-1/2 in. below insert.

[b]Heavy density polyethylene balls.

[c]16 in. of polyethylene (maximum diameter of 28 in.) placed above detector.

[d]Additional polyethylene placed above and alongside the circular pieces.

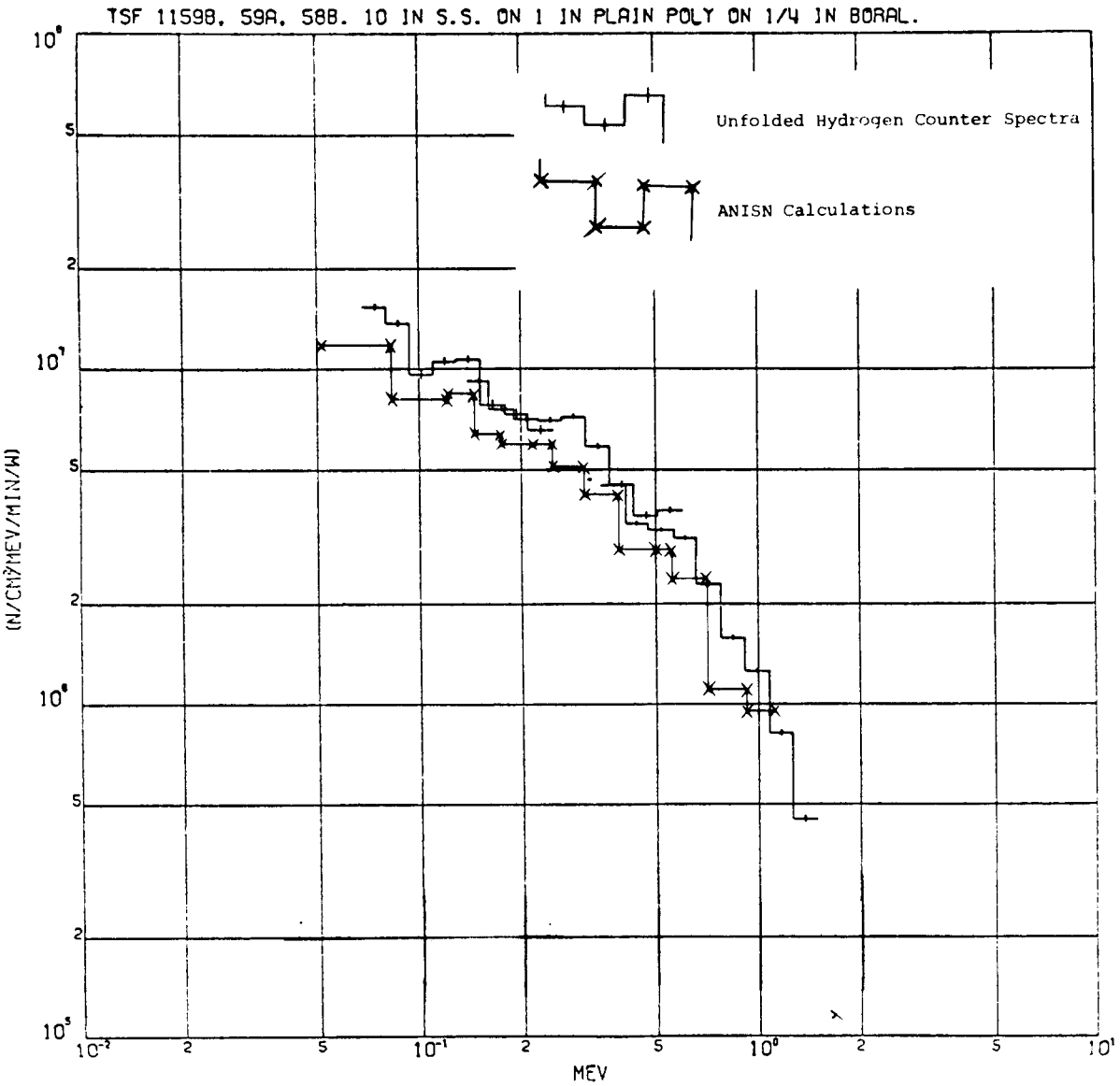

Fig. 15. Comparison of Unfolded Hydrogen Counter Spectra With ANISN Calculations.

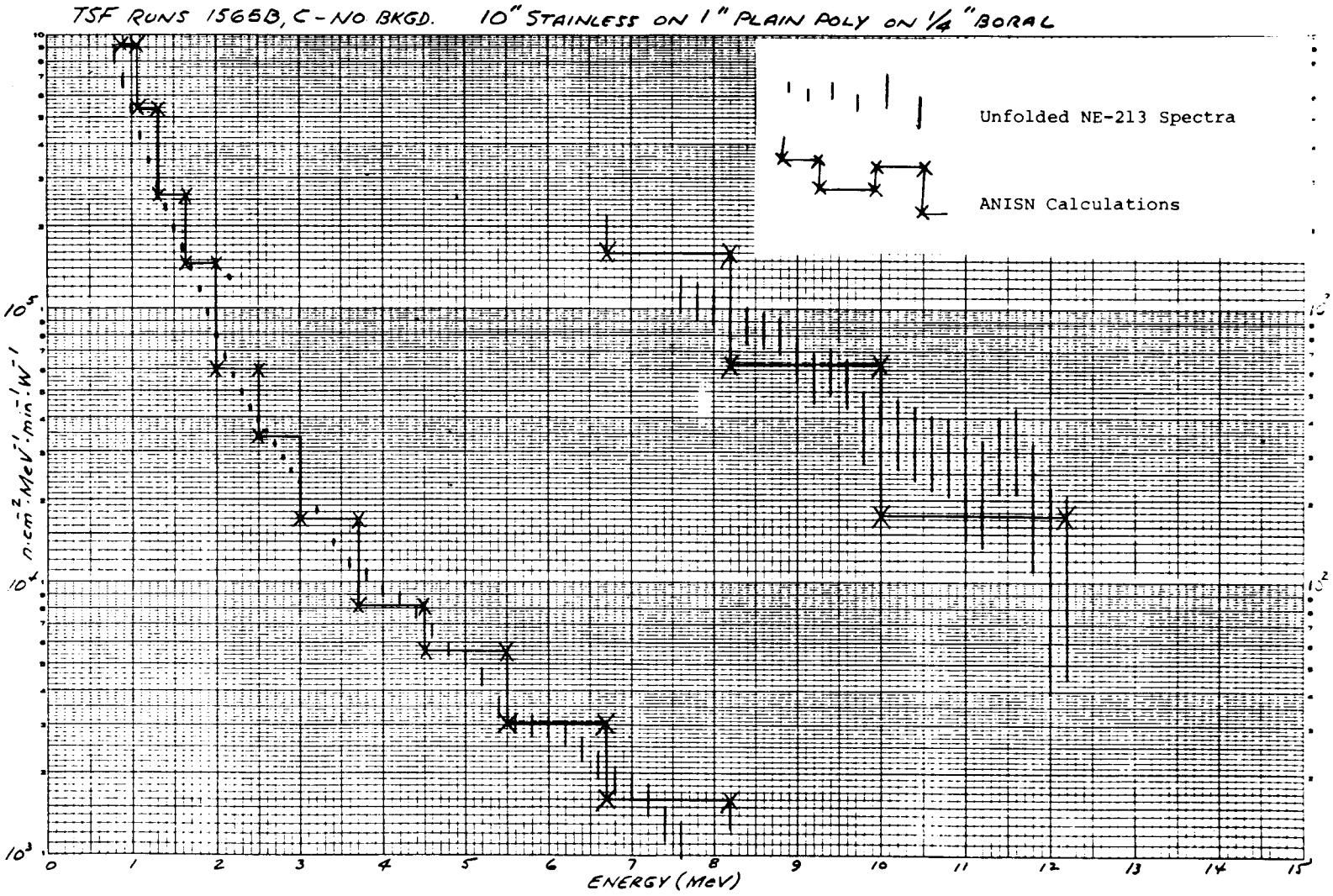

Fig. 16. Comparison of Unfolded NE-213 Spectra with ANISN Calculations.

calculated ANISN results. The ANISN spectrum, presented in Table 3, was normalized to the experimental spectra at 1 MeV so that the comparisons presented are of the spectrum shape only. Absolute comparisons of the modified spectrum have been made utilizing the DOT-III code to calculate the intensity at the detector. The only normalization in the calculation is to the reactor power level. Comparisons of the measured and calculated results on an absolute basis for the hydrogen counter and the NE-213 spectrometer, respectively, are shown in Figs. 17 and 18.

Grid-Plate Shield Inserts - Total-fluence transmission measurements (runs 2-6) were taken for the three grid-plate shield arrangements (inserts 1-3) according to configuration no. 2, as shown in Fig. 10.

Run no. 2 corresponds to the straight-through coolant passages (insert 1). Measurements were taken only on the centerline, the results of which are presented in Table 4. It is noted that the choice of the "O" or "Y" collimator does not significantly alter the transmitted total flux (9522 cpm/W versus 9476 cpm/W, respectively). Comparison with the homogeneous shield (9522 cpm/W for insert 1 and 9093 cpm/W for insert 3) shows a 5% streaming effect. The fractional standard deviation for these runs was less than 1%.

The results for the single-offset coolant passages (run no. 3, insert 2) are presented in Table 5. A comparison of centerline count rates between insert 1 (9522 cpm/W) and insert 2 (9472 cpm/W) shows that there is no appreciable difference between the two arrangements. Comparison with the homogeneous shield (9472 cpm/W for insert 2 and 9093 cpm/W for insert 3) shows a 4% streaming effect. This result is only partially conclusive since the insert no. 2 measurement (9472 cpm/W) had a fractional

Table 3. ANISN Modified-Source Calculations

Group	ΔU (lethargy)	ΔE (MeV)	Upper Energy (MeV)	Differential Flux As Calculated ($n/cm^2/sec/MeV$)	Differential Flux Normalized* to Experimental Spectra at 1 MeV ($n/cm^2/min/MeV/W$)
1	0.2	2.287(-7)	14.92	2.282(-7)	3.64(+1)
2	0.2	1.097(-6)	12.20	1.097(-6)	1.75(+2)
3	0.2	3.932(-6)	10.00	3.932(-6)	6.27(+2)
4	0.2	9.957(-6)	8.19	9.957(-6)	1.59(+3)
5	0.2	1.911(-5)	6.70	1.911(-5)	3.05(+3)
6	0.2	3.492(-5)	5.50	3.492(-4)	5.57(+3)
7	0.2	5.116(-5)	4.50	5.116(-5)	8.16(+3)
8	0.2	1.071(-4)	3.68	1.071(-4)	1.71(+4)
9	0.2	2.159(-4)	3.01	2.159(-4)	3.44(+4)
10	0.2	3.770(-4)	2.47	3.770(-4)	6.01(+4)
11	0.2	9.252(-4)	2.02	9.252(-4)	1.48(+5)
12	0.2	1.625(-3)	1.65	1.625(-3)	2.59(+5)
13	0.2	3.367(-3)	1.35	3.367(-3)	5.37(+5)
14	0.2	5.770(-3)	1.11	5.770(-3)	9.20(+5)
15	0.2	7.145(-3)	0.907	7.145(-3)	1.14(+6)
16	0.2	1.498(-2)	0.743	1.498(-2)	2.39(+6)
17	0.2	1.920(-2)	0.608	1.920(-2)	3.06(+6)
18	0.2	1.885(-2)	0.498	1.885(-2)	3.06(+6)
19	0.2	2.675(-2)	0.410	2.675(-2)	4.27(+6)
20	0.2	3.187(-2)	0.334	3.187(-2)	5.08(+6)
21	0.2	3.700(-2)	0.273	3.700(-2)	5.90(+6)
22	0.2	3.760(-2)	0.224	3.760(-2)	6.00(+6)
23	0.2	4.061(-2)	0.183	4.061(-2)	6.48(+6)
24	0.2	5.280(-2)	0.150	5.28(-2)	8.42(+6)
25	0.2	5.210(-2)	0.122	5.210(-2)	8.31(+6)
26	0.2	8.240(-2)	8.65(-2) 5.25(-2)	8.240(-2)	1.31(+7)

*$(n/cm^2/min/MeV/W) = C*(n/cm^2/sec/MeV)$, where $C = 1.594 \times 10^8$ sec/min/W. The normalized differential flux assumes a value of 9.2×10^5 $n/cm^2/min/MeV/W$ at 1 MeV; the average of the two experimental values at 1 MeV, 5.4×10^5 $n/cm^2/min/MeV/W$ for the NE-213 and 1.3×10^6 $n/cm^2/min/MeV/W$ for the hydrogen counter.

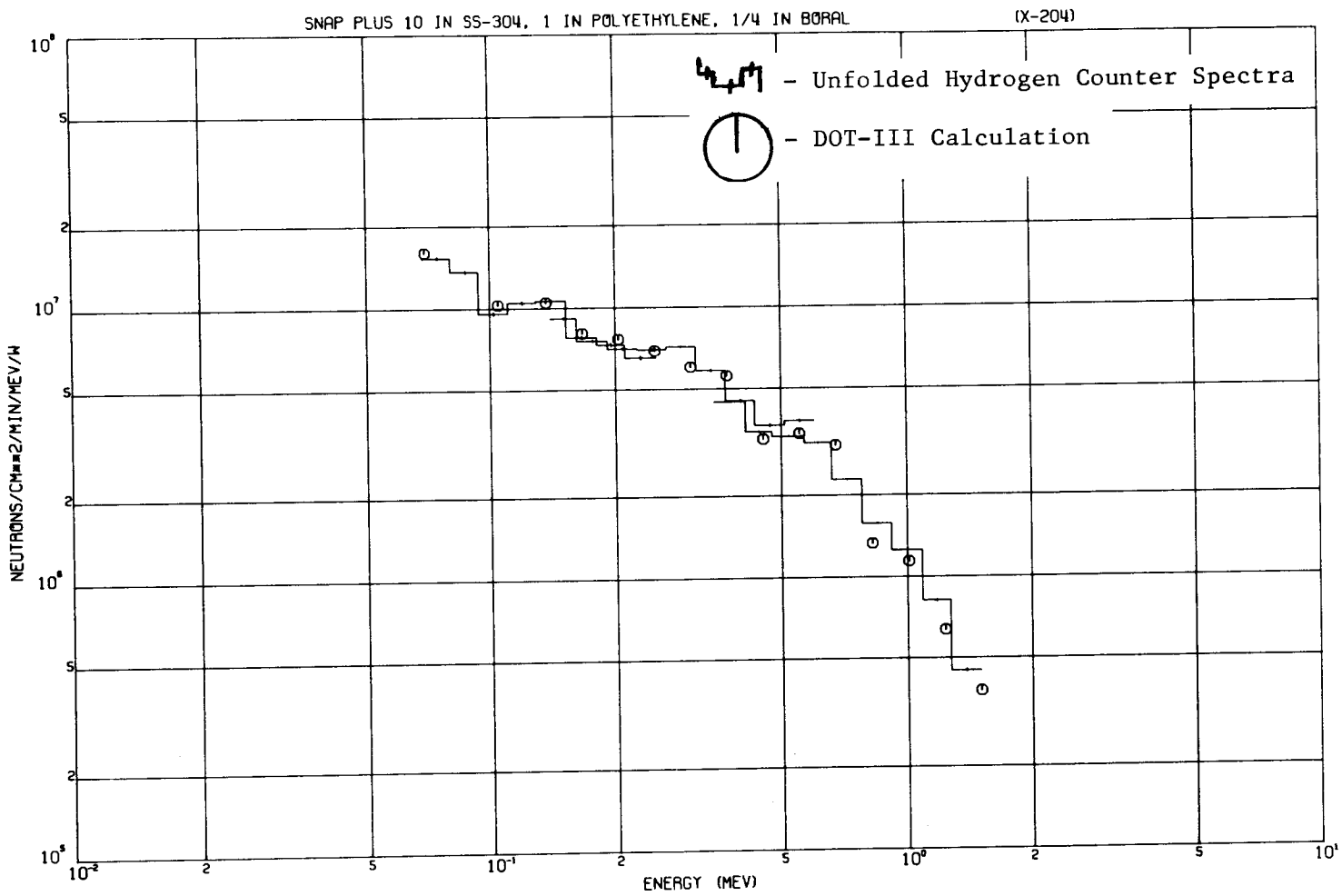

Fig. 17. Comparison of Unfolded Hydrogen Counter Spectra With DOT-III Calculation.

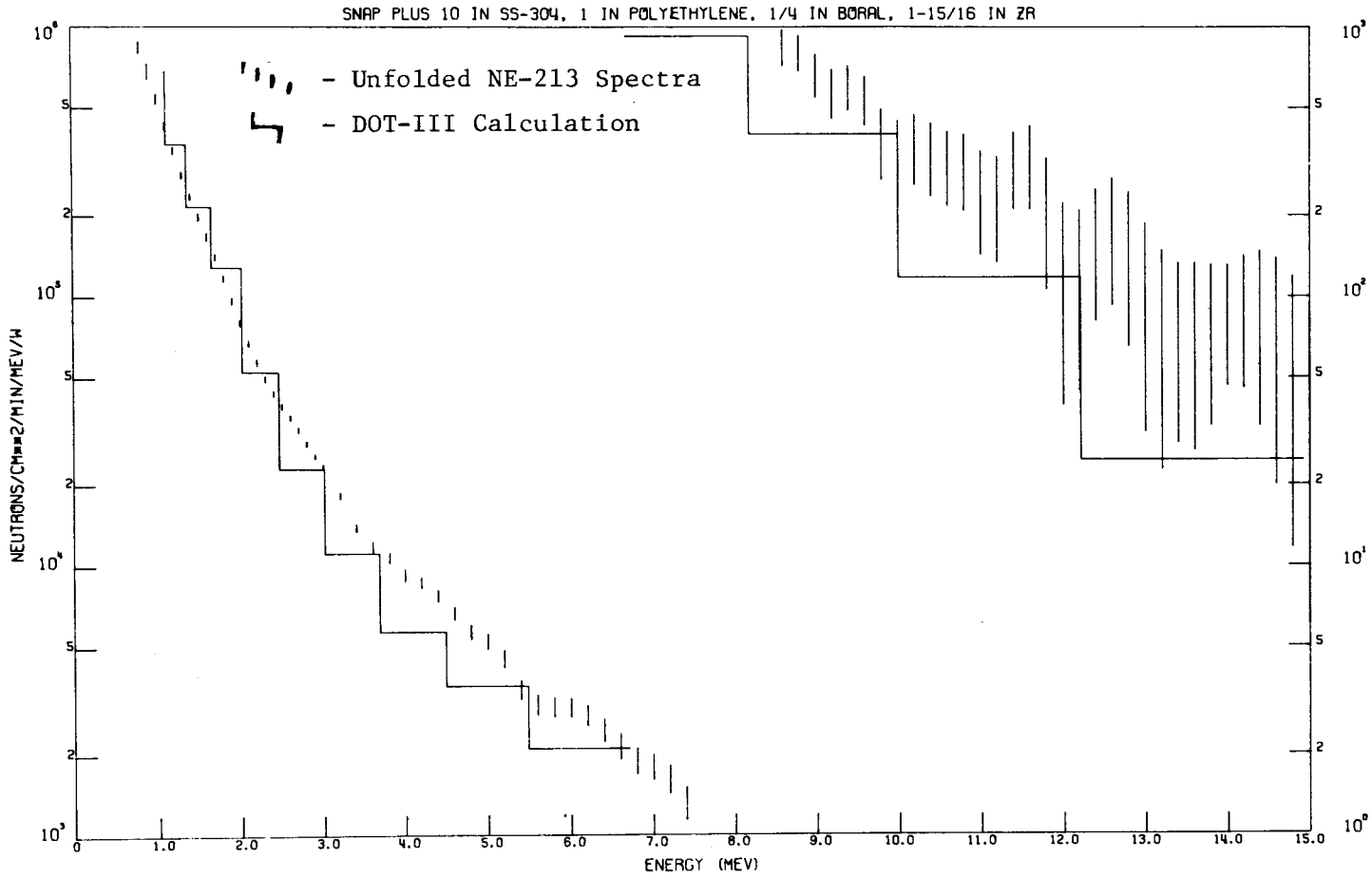

Fig. 18. Comparison of NE-213 Spectra with DOT-III Calculation.

Table 4. Measured 5-in. Bonner Ball Count Rate For Configuration #2 and Insert #1, Run #2

Collimator	Detector Location	(5/18-19/71)	(5/18-19/71)	(5/18-19/71)	Average	FSD* (%)
		(counts/minute/watt)				
0	Centerline	9576	9407	9584	9522	0.625
0	Centerline H_2O	4226	4181	4151	4186	0.528
Y	Centerline	9447	9446	9534	9476	0.308
No Collimator	Centerline	139801	143010	142162	141658	0.675

*Fractional standard deviation associated with the average.

Table 5. Measured 5-in. Bonner Ball Count Rate For Configuration #2 and Insert #2, Run #3

Collimator	Detector Location	(5/13/71)	(5/14-17/71)	(5/17/71)	(5/25-26/71)	Average	FSD* (%)
		(counts/minute/watt)					
Y	H_2O large Y-SW corner	5301	5197	5586	5286	5388	1.76
Y	H_2O centerline	4411	4310	4726	4437	4471	1.98
Y	H_2O small Y-NE corner	4854	4555	5053	4687	4787	2.25
Y	H_2O blank-NW corner	4562	4536	4474	4468	4510	0.52
Y	H_2O small Y-SW corner	4954	4643	4925	4961	4871	1.57
Y	H_2O large Y-NE corner	5474	4953	5317	5170	5229	2.12
Y	Centerline	9163	9255	9890	9581	9472	1.75
0	Centerline	9126	9047	9837	9514	9381	1.95
No collimator	SW corner Y	128149	130721	131734	131848	130613	0.66
No collimator	Centerline	137955	139816	143174	142079	140756	0.83
No collimator	NE corner Y	126655	128131	131914	132305	129751	1.33
No collimator	NW corner, blank	126280	128457	131197	132056	129498	1.02

*Fractional standard deviation associated with the average.

standard deviation of 1.75%, almost the magnitude of the apparent streaming effect. From Table 5 it appears* that the large Y in insert 2 is in the southwest corner. (The streaming factor for the Y-shaped slots is obtained by comparing the measurement for the Y in the collimator lined up with the Y in the shield with a measurement in which the Y in the collimator sees a blank corner of the nearly homogeneous insert.) Thus, the comparison with the Y-collimator measurement for insert 3 (5388 cpm/W for insert 2 and 4953 cpm/W for insert 3) indicates a 9% streaming effect. For the small Y slot, the comparison (4787 for insert 2 and 4664 for insert 3) shows a 3% streaming effect. Again, these comparisons must be judged in comparison with the fractional standard deviation (1.76%) associated with the insert no. 2 measurement.

Run nos. 4, 5, and 6 involve insert no. 3, the insert with a nearly homogeneous arrangement of materials. These results are presented in Tables 6-8, respectively. Run no. 5 provides detailed total flux traverses (mapping) of the emergent face of the homogenized grid-plate shield plus the Y collimator. These data are presented in Table 7 again as (cpm/W). The penetration of the traverse mechanism through the east background shield allowed a significant in-leakage of neutrons. The increased background causes a tilt in the traverse data with the results decreasing from east to west. From comparison of the centerline count rate with that in Table 6 and the magnitude of the east-west tilt, it appears that the background is at least 1000 cpm on the east side and 750 cpm in the center.

The total-flux traverse of run no. 6 involved the homogenized shield without a collimator. These data,presented in Table 8, also show the

---

*In fabrication of the inserts, the location of the Y's was not indicated on the exterior.

Table 6. Measured 5-in. Bonner Ball Count Rates For Configuration #2 and Insert #3, Run #4

Collimator	Detector Location	(5/12/71)	(5/17-20/71)	(5/20/71)	(5/24/71)	Average	FSD* (%)
		(counts/minute/watt)					
Y	Centerline, background	208	-	-	-	208	-
Y	Centerline	9040	9177	9061	-	9093	0.468
Y	H_2O large Y-SW corner	4740	4956	5019	5096	4953	1.55
Y	H_2O small Y-NE corner	4320	4701	4651	4985	4664	2.93
Y	H_2O blank-NW corner	4210	4284	4154	-	4216	0.845
Y	H_2O centerline (corks)	-	4235	4199	4813	4249	0.791
Y	H_2O centerline (tape)	-	-	-	4421	4421	-
0	Centerline	8640	9135	9153	9235	9041	1.50
No collimator	Centerline	137800	138082 & 138700	134616	-	137300	1.150
No collimator	SW corner	127836	124072	126876	-	126261	0.906
No collimator	NE corner	128165	128851	129069	-	128695	0.214
No collimator	NW corner	126945	126106	126914	-	126655	0.214

*Fractional standard deviation associated with the average.

Table 7. Measured 5-in. Bonner Ball Traverse Count Rates For Configuration #2, Insert #3 and "Y" Collimator,[a] Run #5

Detector Location[b]	Count Rate (counts/minute/watt)				
	4-3/32 in. S	2-3/8 in. S	CL	2-3/8 in. N	4-3/32 in. N
17-in. E	3585	3522	3657	3650	3659
8-1/8 in.	5299	5566	5924	5587	5344
4-3/4 in.	7505	8103	8690	8116	7503
2-1/4 in.	8745	9110	9235	8853	8462
Centerline	8670	9439	9684	9107	8324
2-1/4 in. W	8878	9199	9138	8780	8344
4-3/4 in.	7666	7982	8220	7412	6690
8-1/8 in. W	5239	5279	5301	4947	4737
17-in. W	2817	2766	2781	2722	2793
17-in. E*	-	-	3439	-	-
Centerline*	-	-	4650	-	-
17-in. W*	-	-	2553	-	-

[a]Y collimator empty for all measurements except those denoted by "*" for which Y collimator filled with water.

[b]Detector located 3-3/4 in. below collimator.

Table 8. Measured 5-in. Bonner Ball Traverse Count Rates For Configuration #2, Insert #3, No Collimator and Lithiated Paraffin Removed, Run #6

Detector Location (On Centerline in N-S Direction)	Count Rate (counts/minute/watt)
17 in. E	91288
8-1/8 in.	128368
4-3/4 in.	132613
2-1/4 in.	136344
Centerline	136305
2-1/4 in. W	132253
4-3/4 in.	126363
8-1/8 in.	118104
17 in.	79437

effect of neutron leakage through the east wall; however, the value at the center is essentially the same as that given in Table 6. Because of the very low background achieved in the discrete location measurements, such as those given in Table 6, these data are preferred over the traverse data.

The total-flux attenuation of the grid-plate shield is indicated by a comparison of run no. 1 (spectral modifier only) and run no. 4 without the collimator (shield with insert 3). In both of these measurements, the distance from the reactor to the detector was constant so that a direct ratio of the measured values gives a factor of 17 as the attenuation of the shield (2,259,897 cpm/W versus 136,305 cpm/W).

For the shield inserts, the largest streaming factor is given by subtracting the centerline results for the water-filled collimators as a background for the collimated centerline results. For insert 1 this gives 5336 cpm/W, for insert 2 one gets 5001 cpm/W, and for insert 3 one gets 4844 cpm/W. The streaming factor for insert 1 is 10% and for insert 2 it is 3%. Again, these conclusions are somewhat obscured due to fractional standard deviations in the measurements on the order of 2%.

Uncoupled Reactor-Spectrum-Modifier Arrangement - Run no. 7 involves an experimental configuration which is more amenable to diffusion theory analysis. The only measurement taken was the 5-in. Bonner ball count rate, which is considered to be proportional to the total flux. These data are presented in Table 9.

Table 9. Measured 5-in. Bonner Ball Count Rates For Configuration #3 and Insert #3, Run #7

Collimator	Detector Location	Count Rate (cpm/W) (5/26/71)
No collimator	Centerline	97852
No collimator	Centerline	96533
No collimator	Centerline	96533
		96973 (average)

Fractional Standard Deviation associated with the average = 0.456%.

V. SUMMARY

In the assessment of radiation damage effects on the grid plate, the requirement is that the peak total fluence on or within the grid plate must be less than a prescribed value (currently 9.5×10^{21} neutrons/cm^2). Therefore, in considering streaming effects, the peak fluence predicted without streaming must be multiplied by the maximum observed streaming factor for that design in order to obtain the maximum fluence. The lucite collimators were used in order to measure those flux components which were expected to display the largest streaming factors. When the water-filled collimator data are subtracted from the collimateddata, the resulting count rate is due only to neutrons coming through the collimator holes. Using these data, the streaming factor for straight-through coolant passages is 1.10 ± 0.02, and for a single offset the streaming factor is 1.03 ± 0.02. For the Y slots, the collimated data without a water-filled background subtraction show streaming factors of 1.09 ± 0.02 for the larger Y and 1.03 ± 0.02 for the smaller Y.

REFERENCES

1. R. S. Hubner, "Methods for Calculating Fast-Neutron Leakage From the SNAP-TSF Reactor and Preliminary Results," ORNL-TM-1666 (1967).

2. V. R. Cain, "Comparisons of Monte Carlo Calculations to Measurements of Neutron Leakage From the TSF-SNAP Reactor," ORNL-TM-2586 (1969).

3. E. A. Straker, "Measurements of the Absolute Power and Fission Distribution in the TSF-SNAP Reactor and Comparison with Monte Carlo and Discrete Ordinates Calculations," ORNL-TM-2265 (1968); Nucl. Appl. 6, 274-278 (1969).

4. R. E. Maerker, L. R. Williams, F. R. Mynatt, and N. M. Greene, "Response Functions for Bonner Ball Neutron Detectors," ORNL-TM-3451 (1971).

5. P. W. Benjamin, C. D. Kemshall, and J. Redfern, "A High Resolution Spherical Proportional Counter," A.W.R.E. Report No. NR1/64 (1964).

6. C. E. Clifford *et al.*, "Measurements of the Spectra of Uncollided Fission Neutrons Transmitted Through Thick Samples of Nitrogen, Oxygen, Carbon and Lead: Investigation of the Minima in Total Cross Sections," Nucl. Sci. Eng. 27, 299 (1967).

INTERNAL DISTRIBUTION

1-3. L. S. Abbott
4. R. G. Alsmiller, Jr.
5. A. R. Buhl
6. C. E. Burgart
7-11. C. E. Clifford
12. W. W. Engle, Jr.
13. R. M. Freestone, Jr.
14. J. H. Gillette
15. M. L. Gritzner
16. W. O. Harms
17. K. M. Henry
18. L. B. Holland
19. J. L. Hull
20. J. Lewin
21. T. A. Love
22. R. E. Maerker
23. F. C. Maienschein
24. J. J. Manning
25. B. J. McGregor
26. J. N. Money
27. G. L. Morgan
28. F. J. Muckenthaler
29. F. R. Mynatt
30. R. W. Peelle
31. S. K. Penny
32. F. G. Perey
33. A. M. Perry
34. R. W. Roussin
35. H. E. Seagren
36. D. Sundberg
37. D. B. Trauger
38. L. R. Williams
39. H. A. Wright
40. E. R. Cohen (consultant)
41. H. Feshbach (consultant)
42. H. Goldstein (consultant)
43. C. R. Mehl (consultant)
44. H. T. Motz (consultant)
45-46. Central Research Library
47. ORNL Y-12 Tech. Library Document Ref. Section
48-50. Laboratory Records
51. Laboratory Records ORNL RC
52. ORNL Patent Office

EXTERNAL DISTRIBUTION

53. W. H. Hannum, Division of Reactor Development and Technology, U. S. Atomic Energy Commission, Washington, D. C. 20545
54. P. B. Hemmig, Division of Reactor Development and Technology, U. S. Atomic Energy Commission, Washington, D. C. 20545
55. D. F. Cope, USAEC Site Representative, ORNL
56. K. O. Laughon, USAEC Site Representative, ORNL
57. R. Balent, Atomics International, 8900 Desota St., Box 309, Canoga Park, Calif. 91304
58. E. F. Beckett, Project Manager, Westinghouse Electric Corp., Advanced Reactor Division, Waltz Mill Site, P. O. Box 158, Madison, Pa. 15663
59. E. T. Boulette, Radiation & Shield Analysis, WADCO, P. O. Box 1970, Richland, Wash. 99352
60. W. L. Bunch, Radiation & Shield Analysis, WADCO, P. O. Box 1970, Richland, Wash. 99352
61. D. K. Butler, Argonne National Laboratory, 9700 S. Cass Ave., Argonne, Ill. 60439
62-63. E. G. Case, Director, Division of Reactor Standards, U. S. Atomic Energy Commission, Washington, D. C. 20545
64. J. W. Crawford, Division of Reactor Development and Technology, U. S. Atomic Energy Commission, Washington, D. C.
65. R. J. Creagan, Westinghouse Advanced Reactor Division, Waltz Mill Site, P. O. Box 158, Madison, Pa. 15663
66. M. W. Dyos, Westinghouse Electric Corp., Advanced Reactor Division, Waltz Mill Site, P. O. Box 158, Madison, Pa. 15663

67. L. F. Fidrych, General Electric, 310 De Guigne Dr., Sunnyvale, Calif. 94086
68. P. F. Fox, Westinghouse Electric Corp., Advanced Reactor Division, Waltz Mill Site, P. O. Box 158, Madison, Pa. 15663
69. W. E. Fry, U. S. Atomic Energy Commission, P. O. Box 550, Richland, Wash. 99352
70. P. F. Gast, Argonne National Laboratory, 9700 S. Cass Ave., Argonne, Ill. 60439
71. S. A. W. Gerstl, Westinghouse Electric Corp., Advanced Reactor Division, Waltz Mill Site, P. O. Box 158, Madison, Pa. 15663
72. P. Greebler, General Electric Co., Breeder Reactor Development Operation, 310 DeGuigne Drive, Sunnyvale, Calif. 94086
73. P. L. Havenstein, Chief, Instrumentation and Control Branch, U. S. Atomic Energy Commission, Washington, D. C. 20545
74. P. L. Hoffman, Radiation & Shield Analysis, WADCO, P. O. Box 1970, Richland, Wash. 99352
75. T. Iltis, RDT Site Office, U. S. Atomic Energy Commission, P. O. Box 154, Madison, Pa. 15663
76. E. E. Kintner, Division of Reactor Development and Technology, U. S. Atomic Energy Commission, F-309, Washington, D. C. 20545
77. W. Lowenstein, Argonne National Laboratory, 9700 S. Cass Ave., Argonne, Ill. 60439
78. J. J. Morabito, Division of Reactor Development and Technology, U. S. Atomic Energy Commission, Washington, D. C. 20545

79-81. P. A. Morris, Director, Division of Reactor Licensing, U. S. Atomic Energy Commission, Washington, D. C. 20545

82. T. E. Murley, Division of Reactor Development and Technology, U. S. Atomic Energy Commission, Washington, D. C. 20545
83. P. M. Murphy, Manager, Advanced Engineering, General Electric, Sunnyvale, Calif. 94086
84. T. A. Nemzek, U. S. Atomic Energy Commission, P. O. Box 550, Richland, Wash. 99352
85. Prof. P. F. Pasqua, Department of Nuclear Engineering, University of Tennessee, Knoxville, Tenn.
86. T. A. Pitterle, Westinghouse Electric Corp., Advanced Reactor Division, Waltz Mill Site, P. O. Box 158, Madison, Pa. 15663
87. J. L. Rathbun, Westinghouse Electric Corp., Advanced Reactor Division, Waltz Mill Site, P. O. Box 158, Madison, Pa. 15663
88. D. R. Riley, Division of Reactor Development and Technology, U. S. Atomic Energy Commission, Washington, D. C. 20545
89. M. A. Rosen, Division of Reactor Development and Technology, U. S. Atomic Energy Commission, Washington, D. C. 20545
90. W. J. Rowan, Westinghouse Electric Corp., Advanced Reactor Division, Waltz Mill Site, P. O. Box 158, Madison, Pa. 15663
91. M. Shaw, Division of Reactor Development and Technology, U. S. Atomic Energy Commission, Washington, D. C. 20545
92. E. E. Sinclair, Division of Reactor Development and Technology, U. S. Atomic Energy Commission, Washington, D. C. 20545
93. B. J. Snyder, Division of Reactor Development and Technology, U. S. Atomic Energy Commission, Washington, D. C. 20545
94. P. N. Stevens, Oregon State University, Radiation Center, Corvallis, Oregon 97331

95. E. R. Specht, Atomics International, 8900 Desota Street, Box 309, Canoga Park, Calif. 91304
96. D. C. Spencer, Westinghouse Electric Corp., Advanced Reactor Division, Waltz Mill Site, P. O. Box 158, Madison, Pa. 15663
97. W. P. Staker, Manager, Fast Breeder Development, Combustion Engineering, Windsor, Conn. 06095
98. D. G. Stenstrom, Argonne National Laboratory, 9700 S. Cass Ave., Argonne, Ill. 60439
99. A. N. Tardiff, Division of Reactor Development and Technology, U. S. Atomic Energy Commission, Washington, D. C. 20545
100. J. Taylor, General Manager, Westinghouse, Advanced Reactor Division, Waltz Mill Site, P. O. Box 158, Madison, Pa. 15663
101. M. L. Weiss, General Electric Co., Breeder Reactor Development Operation, 310 DeGuigne Drive, Sunnyvale, Calif. 94086
102-103. Division of Technical Information Extension (DTIE)
104. Laboratory and University Division (ORO)